Materials Characterization 145 (2018) 413–422

Contents lists available at ScienceDirect

Materials Characterization

journal homepage: www.elsevier.com/locate/matchar

Precipitation behavior of Widmanstätten O phase associated with interface in aged Ti_2AlNb-based alloys

Qi Cai[a], Mengchen Li[b], Yaran Zhang[b,*], Yongchang Liu[b,*], Zongqing Ma[b], Chong Li[b], Huijun Li[b]

[a] Materials Genome Institute, Shanghai University, 333 Nanchen Rd, Shanghai 200444, China
[b] State Key Laboratory of Hydraulic Engineering Simulation and Safety, School of Materials Science and Engineering, Tianjin University, Tianjin 300354, China

ARTICLE INFO

Keywords:
Ti_2AlNb alloys
Ball milling
Ageing
Hardness
Interface

ABSTRACT

Ti_2AlNb-based alloys, spark plasma sintered from ball-milled octahedral Ti-22Al-25Nb powder, are aged for 0–3 h in this study. Ball milling tunes the morphology of primary orthorhombic (O) phase to be columnar, and improves the mechanical properties of the alloys. The evolution of the Widmanstätten O phase, which brought main precipitation strengthening effect, is then investigated during the ageing process. The hardness of the alloys is improved by an increasing content of O phase and the reduced width of the Widmanstätten O phase; in addition, the length of Widmanstätten O phase also brings positive effect on the hardness, which indicates that the hardness is strongly coupled with the interface of the Widmanstätten O precipitates and B2 matrix. By means of transmission electron microscopy observation, the precipitation of O initials with an amorphous state, followed by a coherent interface between $(110)_{B2}$ and $(002)_O$, which is destroyed to be semi-coherent and incoherent during the next ageing stage.

1. Introduction

Materials with excellent high-temperature strength, creep rupture life, and corrosion resistance, are considerably desirable in the aeronautic and aerospace fields. Ti_2AlNb-based alloys, featured by an orthorhombic (O) phase, are regarded as promising candidates for conventional Ti_3Al alloys, which suffer low fracture toughness at room temperature [1–3]. However, Ti_2AlNb may experience complicated microstructure evolution during hot working, as well as a variety of phase transformation, associated with multiple phases of B2 (ordered body-centered cubic, bcc), α_2 (hexagonal close-packed, hcp), and O (orthorhombic) [4–6]. The resultant fluctuation of mechanical properties might lead to failure of the alloys.

Studies have addressed on the Ti_2AlNb-based alloys prepared by mechanical alloying from elementary powder or Ti-22Al-25Nb pre-alloyed powder, which is desirable to directly produce Ti_2AlNb components of a complex shape without superfluous cutting and processing, and the microstructure dependence of mechanical properties have been intensely investigated during ageing or continuous cooling [7–9]. Niu et al. have reported that fine acicular O phase is favorable to the tensile strength, whereas appropriate coarsening of O phase on the other hand improved the ductility of the Ti_2AlNb-based alloys [10]. Sim et al. have prepared Ti_2AlNb-based alloys with a combination of fine B2 grains, ultrafine equiaxed α_2, and acicular O precipitates by high-energy ball milling, and the compression strength exceeded that of the alloys containing coarse grains and precipitates [11]. Our previous study has shown that ball milling induced acicular O phase, rather than B2 + O colonies, in the B2 matrix to bring about precipitation strengthening for improved mechanical properties [12]. Similar trials by Sim et al. have also [13] proved that a moderate milling time enhanced the tensile properties by increasing the dislocation density, in addition to the precipitation of O phase and the grain refinement. Hence, fabrication of Ti_2AlNb-based alloys from pre-alloyed Ti-22Al-25Nb is a feasible method to prepare a finely grained or precipitation strengthened Ti-22Al-25Nb alloy.

The essential limit in the application of Ti_2AlNb-based alloy is the poor ductility and toughness [14]. However, coarse O contributes to the ductility by sacrificing the strength, and acicular O introduces stronger strengthening effect, yet depresses the ductility [15]. When the alloys are solution treated and quenched from high temperature in the B2, B2 + α_2, or B2 + α_2 + O phase region, a mixed structure of B2 and α_2/O, with equiaxed or lamellar α_2/O in the B2 matrix, is obtained [6]. A subsequent ageing treatment in the B2 + O phase region may lead to the precipitation of acicular O phase within the B2 grains, forming Widmanstätten structure [16], and the primary O remains relatively unchanged during ageing [15]. The primary coarse O contributes to the creep resistance, while the fine Widmanstätten O exhibits better strengthening effect [17]. The primary O phase can be regulated by

* Corresponding authors.
E-mail addresses: caiqi@shu.edu.cn (Y. Zhang), ycliu@tju.edu.cn (Y. Liu).

https://doi.org/10.1016/j.matchar.2018.09.009
Received 7 August 2018; Received in revised form 6 September 2018; Accepted 6 September 2018
Available online 07 September 2018
1044-5803/

tailoring the fabrication technique, and the Widmanstätten O phase can be controlled by using appropriate ageing conditions. In view that the mechanical properties of Ti_2AlNb-based alloys rely mostly on the Widmanstätten O precipitates, it is also necessary to clarify the precipitation mechanism of the Widmanstätten O phase, under the used fabrication technique and the applied heat treatment.

In this study, pre-alloyed spherical and ball-milled octahedral Ti-22Al-25Nb powders are used to fabricate Ti_2AlNb-based alloys. After typical solution treatment and ageing stages, the morphology of O-phase precipitates in Ti_2AlNb-based alloys is expected to be regulated by the introduced milling stage, accompanied by a simultaneous enhancement of strength and ductility. Furthermore, the microstructure evolution is investigated during the ageing process, and a relation among the phase composition, microstructure, and hardness is constructed for the alloys from ball-milled powder. On this basis, the formation mechanism of O phase in the alloys from ball-milled powder is interpreted by comparing with the mechanism in the alloys from pre-alloyed powder.

2. Experimental Details

Ti-22Al-25Nb (at.%) ingots (Φ560 mm) were melted from element powder in a vacuum arc melting furnace for three times, and were forged six times to obtain bars (Φ60 × 700 mm). Spherical pre-alloyed powder was then produced from these bars by argon gas atomization using plasma heat source under dc signal. The rotation speed is 16,000 r/min. The pre-alloyed powder (single B2 phase, Fig. 1a) was milled for 100 h in a high energy ball mill, with the rotation speed of 360 rpm and under the protection of Ar gas. The ball to powder ratio was 30:1. The un-milled and milled powders were then spark plasma sintered (SPS, Dr. Sinter SPS-625, Fuji Electronic Industrial Co. Ltd.) at 1100 °C for 10 min at a pressure of 50 MPa. The porosity is estimated to be 1.20% and 0.71% for the alloys SPSed from pre-alloyed and ball-milled powder, respectively. The as-sintered alloys were solution treated at 1100 °C (single B2 phase region) for 1 h, followed by water quenching, and aged at 800 °C (B2 + O phase region) for 0.5 h, 1 h, 2 h, and 3 h, followed by air cooling. The SPSed alloys from pre-alloyed powder were solution treated at 1100 °C for 1 h, followed by water quenching, and aged at 800 °C for 0.5 h, 1 h, 2 h, and 3 h. The sintering temperature, 1100 °C, falls in the single B2 phase region, according to the Ti-22 at.% Al-*x*Nb phase diagram [6]. It is expected to avoid the phase transformation during the SPS process, so the powder (B2 phase) is sintered in single B2 phase region. Ageing temperature falls in the B2 + O phase region to obtain a mixture of B2 + O Widmanstätten microstructure.

The phase composition of the powder and the sintered alloys was examined by X-ray diffraction (XRD, Bruker D8 Advanced) using Cu Kα radiation, and the microstructure was characterized by scanning electron microscopy (SEM, Hitachi S-4800) and transmission electron microscopy (TEM, JEM-2100f). The room temperature microhardness was measured by the Vickers hardness test (0.2 kg load) according to the ASTM E18–94 standard. The room temperature tensile tests were performed on an Instron 5848 tensile machine at a strain rate of $0.04\ min^{-1}$. The marked length and width of each minor specimen were 5 mm and 1.5 mm, respectively.

3. Results and Discussion

3.1. Microstructure and Mechanical Properties of Alloys From Pre-alloyed and Ball-milled Powder

The milled powder remained in single B2 phase with ordered bcc structure, according to the XRD pattern in Fig. 1a, and the powder that suffered mechanical breakage was prone to exposing the {111} crystal planes, which are the densest ones in bcc crystals, resulting in an octahedral shape for these milled particles (insets of Fig. 1a). According to the XRD patterns, the full width at half maximum (FWHM) of the (110), (211), and (220) peaks for B2 phase is illustrated in Fig. 1b. The increasing FWHM for all the crystal planes of B2 phase indicates that the milled powder is composed of smaller B2 grains than the pre-alloyed one, and the milled powder accumulates micro-strain in the lattice scale, due to the stored energy during ball milling. Moreover, the average particle size is 230.6 ± 29.3 μm and 142.4 ± 45.4 μm for pre-alloyed and ball-milled powder, respectively, as shown in Fig. 1c. The particle size distribution for the pre-alloyed and ball-milled Ti-22Al-25Nb powder is shown in Fig. 2. Besides the refinement, the size of the particles distributes in a narrower range for the ball-milled powder, in contrast with the pre-alloyed one. The distinction between the powders is likely to result in an alternative precipitation of the O phase in the alloy prepared from milled powder.

The XRD patterns of the Ti_2AlNb alloys aged for 0.5 h from the pre-alloyed and milled powder are illustrated in Fig. 3a. The SPSed alloy from pre-alloyed powder consists of dual B2 and O phase, whereas pre-milling of the powder induces extra α_2 phase. It is also recognized an

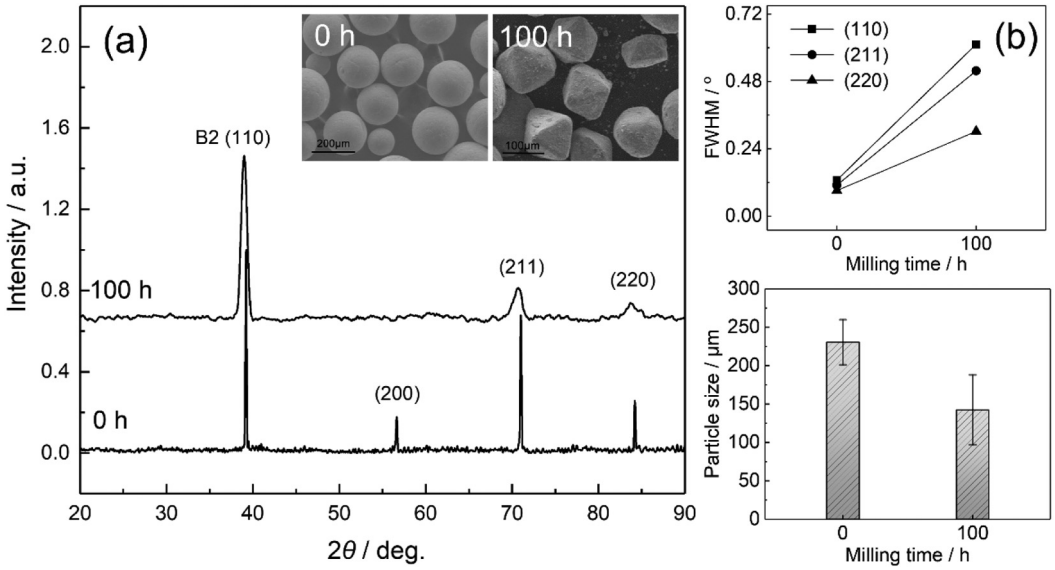

Fig. 1. (a) XRD patterns and SEM images (insets) of pre-alloyed and ball-milled powder, (b) calculated FWHM of the peaks corresponding to B2 phase in the powder, and (c) average particle size of pre-alloyed and ball-milled powder. The counts of the XRD patterns are normalized.